



Cite this: DOI: 10.1039/d0dt01809k

Photoresponsive Zn²⁺-specific metallohydrogels coassembled from imidazole containing phenylalanine and arylazopyrazole derivatives†

Ashanti Sallee and Kesete Ghebreyessus *

Stimuli-responsive supramolecular gels and metallohydrogels have been widely explored in the past decade, but the fabrication of metallohydrogels with reversible photoresponsive properties remains largely unexplored. In this study, we report the construction of photoresponsive hybrid zinc-based metallohydrogel systems coassembled from an imidazole functionalized phenylalanine derivative gelator (ImF) and carboxylic acid functionalized arylazopyrazole (AzoPz) molecular photoswitches in the presence of Zn²⁺ ions. Unlike traditional covalent conjugation, noncovalent introduction of small molecular switches into the gel matrix provides a convenient route to generate photoresponsive functional materials with tunable properties and expands the scope of optically controlled molecular self-assemblies. It has been found that the carboxylic acid functionalized AzoPz derivatives alone or mixed with the ImF moiety could not self-assemble to form any gels. However, in the presence of Zn²⁺ ions they readily formed the coassembled hybrid metallohydrogels in an alkaline aqueous solution with various morphologies. These results suggest that the gelation process was triggered by the Zn²⁺ ions. In addition, the ImF gelator shows specific response to Zn²⁺ ions only. The presence of the AzoPz moiety in the gel matrix makes the metallohydrogel coassemblies photoresponsive and the reversible gel-to-sol phase transition was studied by UV-vis spectroscopy. The gels showed a slow reversible light-induced gel-to-sol phase transition under UV ($\lambda = 365$ nm) and then sol-to-gel transition by green light ($\lambda = 530$) irradiation resulting in the reformation of the original gel state. The morphology and viscoelastic properties of the fibrillar opaque metallohydrogels have been characterized by transmission electron microscopy (TEM) and rheological measurement, respectively.

Received 19th May 2020,
Accepted 6th July 2020
DOI: 10.1039/d0dt01809k

rsc.li/dalton

Introduction

Stimuli-responsive supramolecular gels formed from low-molecular-weight gelators (LMWGs) have emerged as a promising class of soft materials, in part, due to their potential applications in chemical sensing,^{1–5} tissue engineering,^{6–8} switchable catalysis,^{9–11} environmental remediation,^{12–14} drug delivery^{15–18} and other materials science fields. The main driving forces for LMWG molecules to self-assemble into nano-scale structures are generally weak noncovalent interactions involving hydrogen bonding, π - π stacking, hydrophobic interactions and coordination interactions^{19–23}. Recently, metal-induced gelation of LMWGs has also been recognized as a promising strategy for the fabrication of gels with multiple stimuli sensitivity by tuning the dynamic metal-ligand coordi-

nation.²⁴ The incorporation of metal-ions into the supramolecular assembly can enrich the properties of these soft materials with metal specific functionality such as optical, magnetic, electronic, luminescence, and enhanced catalytic properties.²⁵ To date, a variety of metallohydrogels based on metal ion coordination with various organic ligands, amino-acids and peptides have been reported.^{24–29} The dynamic and reversible nature of the metal-ligand coordination make the metallohydrogels responsive to a variety of stimuli such as pH, temperature, chemical species and light.^{24e,f,25} Among these, metallohydrogels that incorporate photoresponsive functionalities are particularly attractive owing to their potential to design adaptive hybrid soft materials with tunable gelation properties by light-irradiation.

Normally, the construction of light-responsive metal-ligand supramolecular assemblies is achieved through the incorporation of photochromic compounds in the structure of their ligands. Irradiation with a specific wavelength of light enables alteration of the conformation of the photochromic ligand, which in turn may result in a structural reconfiguration of the metallohydrogel assembly.²⁶ However, the fabrication of photore-

Department of Chemistry and Biochemistry, Hampton University, Hampton, VA, 23668, USA. E-mail: Kesete.Ghebreyessus@hamptonu.edu; Tel: +1-757-727-5475

† Electronic supplementary information (ESI) available: Synthetic route, ¹H and ¹³C NMR spectra, UV-Vis spectra, optical pictures, IR spectra and mass spectra. See DOI: 10.1039/D0DT01809K

sponsive metal–ligand assemblies that incorporate photochromic ligands in their supramolecular structure is not straightforward. The design of suitable photochromic ligands that coordinate with metal ions and self-assemble to form gels often requires substantial time and complicated synthetic efforts. An alternative but relatively unexplored approach to make metal–ligand assemblies light-responsive is through the noncovalent introduction of photoswitchable moieties to form metallogels *via* controllable coassembly.^{26b} This approach may provide a simple and efficient method to introduce functional moieties to the molecular structure and enables reversible photo-modulation of nonphotoresponsive supramolecular assemblies. Most of the gels described in the literature thus far are obtained from single-component LMWGs in aqueous or organic medium; however, some are formed from multi-component coassemblies using the supramolecular approach.^{6,30–38} Compared to the single-component gels, the two/multi-component gels provide the possibility to create hybrid soft materials with diverse and tunable properties through the noncovalent introduction of different functional units within a single gel.^{30–38} Furthermore, the properties of the gels can be controlled by varying the molar ratios of the different components. Despite this, the preparation of two/multi-component gels that contain metal centers remains largely unexplored.^{26b} In particular, the photoresponsive gel-to-sol phase transitions in two-component gels have rarely been extended to the study of metal–organic hybrid soft materials.^{26b} This leaves scope to explore the photoswitchable behavior of metallogels suitably designed through the two/multi-component approach, which is the goal of the present study.

To date, azobenzene and its derivatives are the most widely used switchable molecules that have been integrated into metallosupramolecular structures, host–guest coordination cages, polymers and peptides for the development of photoresponsive self-assembly systems owing to their reversible *trans*-to-*cis* isomerization in response to UV light.^{39–41} This photo-induced isomerization results in a *cis*-isomer with a shorter length scale and can lead to macroscopic change in the corresponding materials. Despite this, azobenzenes also suffer from two major photoswitch performance issues: incomplete photo-switching at a given wavelength of light and low thermal stability of the *cis* isomer. In this context, arylazopyrazoles (AzoPzs) have been recently introduced as improved light-responsive molecular switches compared to their azobenzene counterparts.⁴² AzoPzs represent novel yet, largely unexplored emerging molecular switches. AzoPzs have recently been found to undergo better light-triggered reversible *trans*-to-*cis* isomerization compared to the commonly used azobenzene derivatives by virtue of their heteroaromatic rings.^{42a–c} Recently, the potential applications of these new molecular switches have been explored further for the development of several supramolecular systems ranging from host–guest complexes, foams, adhesives, DNA complexes, light-responsive peptide hydrogels with host–guest interactions and coordination complexes.^{42c,e,f,43} It is the aim of this article therefore to exploit these unique properties of AzoPzs for the development

of new photoswitchable metallohydrogels that would enable the reversible photomodulation of the gels' physicochemical properties.

In this study, we report the fabrication of a photoresponsive zinc-based metallogel system coassembled from an imidazole-substituted phenylalanine derivative LMWG ligand (ImF) and carboxylic acid functionalized arylazopyrazole (AzoPz) small molecular switches in the presence of Zn²⁺ ions in alkaline aqueous solution at pH ~ 11.00 (Fig. 1). Vortex treatment of the initial turbid mixtures of the compounds and the presence of Zn²⁺ ions were found to be critical factors for the supramolecular assembly and formation of stable metallogels. Out of the different metal salts that were tested, stable metallogels are selectively formed in the presence of zinc salts only. It is to be noted that although the construction of La³⁺-based metallohydrogels using the ImF gelator has been recently reported,^{27c} the design of light-responsive metallogels utilizing the ImF LMWG have not been described before. The ImF can serve as an excellent LMWG ligand to fabricate metallogels because it possesses two N-atoms for metal-ion coordination and provides rich non-covalent interactions such as hydrogen-bonding and π - π stacking interactions.^{27c} The three molecular photo-switches described in Fig. 1 below has been chosen because of their moderate solubility in water and ease of synthesis. The three compounds contain carboxylic acid groups covalently linked at different positions of the AzoPz moiety. The purpose of this strategy was to explore if the subtle structural changes in the molecular switches would lead to distinct coassembled gels. The presence of the carboxylic acid functional groups in the AzoPz units can induce noncovalent hydrogen-bonding interaction and provide metal-coordinating sites through the *N*-pyrazole ligand which could facilitate the formation of stable gels. Furthermore, the presence of the phenylalanine group from ImF provides the possibility of tuning the self-assembly through π - π stacking and by adjusting the pH and further enhances gelation ability.^{6,45} Owing to the presence of the photoswitchable azo moiety, the resulting metallogels displayed slow reversible light-induced gel-to-sol phase transitions upon alternating UV and green light irradiation. The light-responsiveness property and morphological features of the metallogels could be tuned by varying the substitution patterns of the carboxylic acid functionalized AzoPz molecular switches.

Results and discussion

Synthesis and characterization

Synthesis of AzoPz1–3. The small molecular azo switch derivatives, AzoPz1–3, were synthesized following standardized literature procedures.^{42a,f,44} Starting from commercially available aniline derivatives, AzoPz1–2 were synthesized in a simple three-step procedure (Scheme S1†). First, the 4-ethyl-amino-benzoate derivative was converted into the diazonium salt by hydrochloric acid and sodium nitrite, which was subsequently reacted *in situ* with 2,4-pentandione to afford the precursor

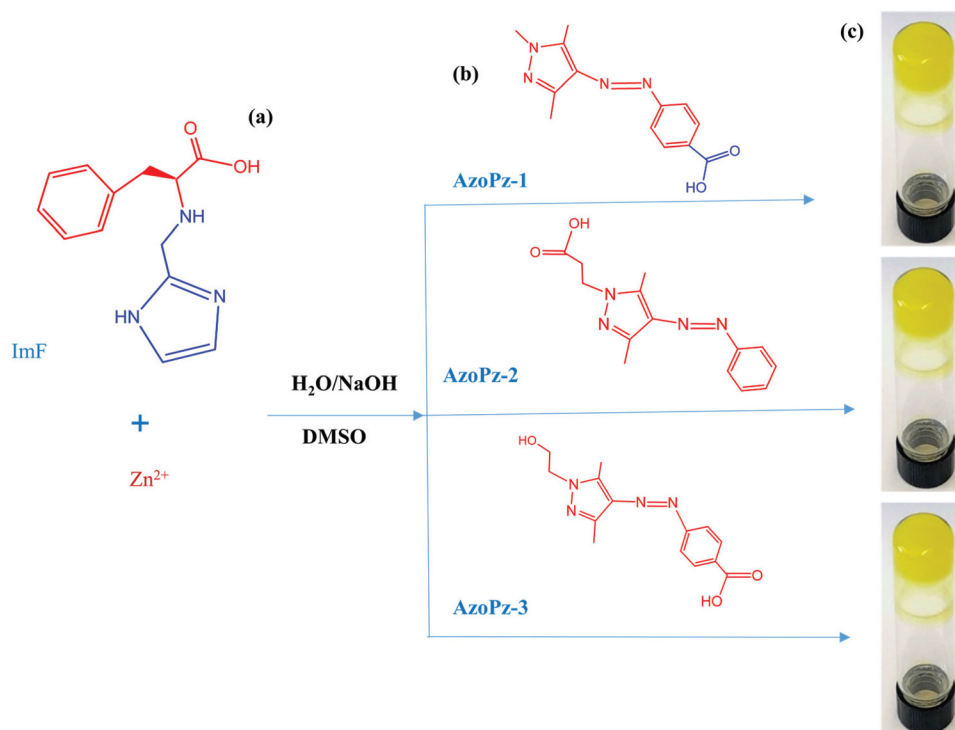


Fig. 1 (a) Chemical structure of the ImF gelator; (b) molecular structures of the AzoPz-1, AzoPz-2 and AzoPz-3 photoswitches; (c) pictures of glass vials containing the metallogel coassembled by the Zn^{2+} ion triggered self-assembly of ImF (MGC of 0.05 M) and the three photoswitchable azo compounds at room temperature.

hydrazones as yellow solids in high yield (**1a**). The reaction of the resulting hydrazones with substituted hydrazines under reflux conditions afforded the corresponding intermediate compounds (**2a** and **3a**). Base hydrolysis of the resulting intermediate compounds afforded the desired AzoPz1–2 molecular switches in quantitative yield. Details of the synthesis and analysis of all the AzoPz1–2 are provided in the ESI, Scheme S1.† AzoPz-3 can also be obtained by simple substitution and hydrolysis reactions of the intermediate compounds (**1b–3b**) as another series of azo switch (see the ESI, Scheme S2†). All the compounds have been characterized by ^1H NMR, ^{13}C NMR, and UV-vis spectroscopy. Similar to previously reported AzoPz based photoswitches, the presence of the characteristic peaks of the CH_3 group of the pyrazole moieties in the 2.50–2.60 ppm range in the NMR spectra indicates that, in all cases, the molecular switches exist in their more stable *trans* isomers under normal conditions.⁴²

Synthesis of N-(1-H-imidazol-2-yl)methylidene-L-phenylalanine (ImF). The synthesis of the imidazole (Im) containing the phenylalanine (Phe) derivative gelator, abbreviated as ImF, is achieved by a condensation reaction between Phe and Im to afford the intermediate imine product (**1c**) as shown in the ESI, Scheme S3.†^{27c} Subsequent reduction of the imine intermediate product (**1c**) with NaBH_4 at 0 °C afforded the corresponding N-(1-H-imidazol-4-yl)methylidene-L-phenylalanine (ImF) as a white solid in high yield. The resulting compound has been characterized by ^1H NMR, ^{13}C NMR and Fourier

transform infrared (FTIR) spectroscopy. The ^1H NMR spectrum of ImF shows peaks in the aromatic region ranging from 7.40 to 7.05 ppm and the aliphatic protons 3.77–2.94 ppm. The ImF compound was isolated as a white solid with good solubility in alkaline aqueous solution.

Gelation study

To test the gelation behavior of the imidazole substituted phenylalanine based gelator (ImF), we first examined the self-assembly of a series of metal ions such as Ca^{2+} , Ni^{2+} , Pb^{2+} , Cu^{2+} , Zn^{2+} , and Mn^{2+} at room temperature (see the ESI, Fig. S15†). The gelation studies were carried out by mixing an alkaline solution of ImF and aqueous metal salt solutions by vortex treatment. The results show that only Zn^{2+} induces the formation of a stable self-standing metallogel, indicating that the ImF gelator is Zn^{2+} selective. Upon mixing the two components, the solution immediately turned turbid and transformed into an opaque white metallogel after vortex treatment for 10 min which was confirmed by the test tube inverting method (Fig. 2). Meanwhile no gel formation was observed without vortex treatment upon standing of the turbid mixture for several hours at room temperature. Application of vortex treatment to the initial turbid mixture was found to be a critical step in the self-assembly process and for the formation of a stable metallogel. It is also important to mention that the ImF gelator did not form any gel by itself under an alkaline solution at $\text{pH} \sim 11.0$. However, the combination of

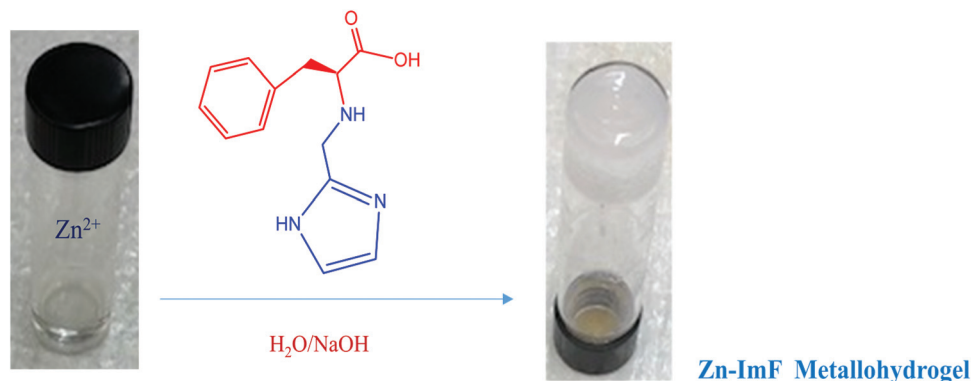


Fig. 2 Preparation of the Zn^{2+} -triggered Zn–ImF metallohydrogel at the MGC of 0.07 M at room temperature.

the alkaline solution of ImF and aqueous solution of $ZnCl_2$ produced an opaque white metallohydrogel, indicating the critical role played by the Zn^{2+} ions in the gelation process. The effect of anions on gelation was further examined by using $ZnSO_4$, $Zn(NO_3)_2$, and $Zn(OAc)_2$ under the same conditions. All zinc salts formed white metallohydrogels upon mixing alkaline solutions of the ImF (pH ~ 11.0) gelator with Zn^{2+} in a 2 : 1 molar ratio of Zn^{2+} ions and ImF with a minimum gelation concentration of 0.07M (see Table S1 and Fig. S14 in the ESI[†]). These results indicate that anions of the metal salt have no significant influence on the formation of the gels. The formed metallohydrogels were fairly stable, as no disruption of the gel was observed upon standing for several months.

Coassembly of ImF with Zn^{2+} and arylazopyrazole (AzoPz) derivatives

The gelation properties of the coassembly system were tested in a manner similar to that of the Zn^{2+} –ImF gels. As noted above, the ImF gelator alone or in combination with the AzoPz photo-switches could not self-assemble to form any gel even after vortex treatment. However, the combination of the alkaline solution of ImF with aqueous solution of Zn^{2+} salts and AzoPzs dissolved in a minimum amount of dimethylsulfoxide (DMSO) resulted in the formation of stable yellow colored metallohydrogel coassemblies after vortex treatment (Fig. 3). The minimum gelator concentration (MGC) was found to be 0.05

M when the molar ratio of ImF, Zn^{2+} and AzoPzs was 2 : 1 : 0.5 at room temperature. It should be noted that before mixing, the pH of the ImF solution was adjusted to pH ~ 11.0 by using 1 M NaOH. Successful formation of the gels was confirmed by the inverted test tube method, which did not show fluid flowing down lasting for at least 30 min. All the investigated carboxylic acid substituted AzoPz derivatives resulted in the facile formation of a yellow colored metallohydrogel with ImF in the presence of Zn^{2+} ions. We also tested different mole ratios of Zn^{2+} and AzoPz to the ImF moiety following a similar procedure, but no gels could be obtained.

Transmission electron microscopy (TEM) study

To further investigate the morphological features of the metallohydrogel coassembly obtained from Zn–ImF and Zn–ImF–AzoPzs, transmission electron microscopy (TEM) images of the gels were recorded. The TEM images of the different metallohydrogels are shown in Fig. 4. These images reveal that the Zn–ImF gel without the AzoPz photoswitches forms fine intertwined nanofibrillar network structures with an average diameter of $\sim ca.$ 30 nm and several micrometers (μm) long (Fig. 4a). The morphology of the hybrid gels, formed from the Zn–ImF–AzoPzs' coassembly (Fig. 4b–d), was similar to that of the Zn–ImF metallohydrogel, but it was also possible to discern some difference in terms of the length and diameter of the nanofibers. The Zn–ImF–AzoPz-1 gel was comprised of a long

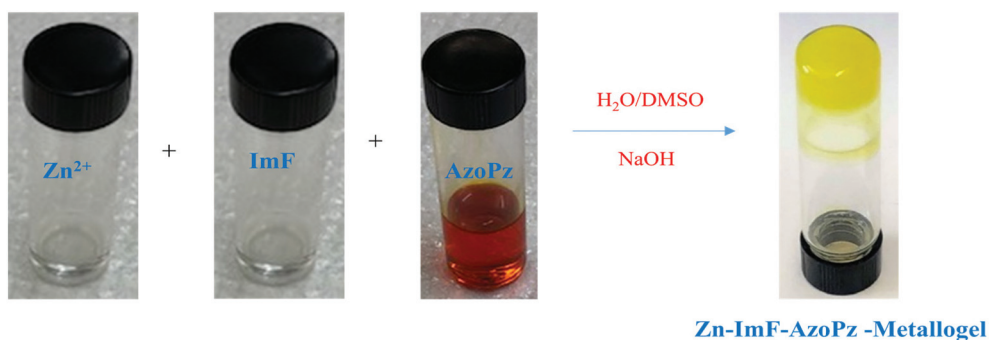


Fig. 3 Coassembly of Zn^{2+} -triggered formation of the photoresponsive Zn–ImF–AzoPz metallohydrogels at the MGC of 0.05 M at room temperature.

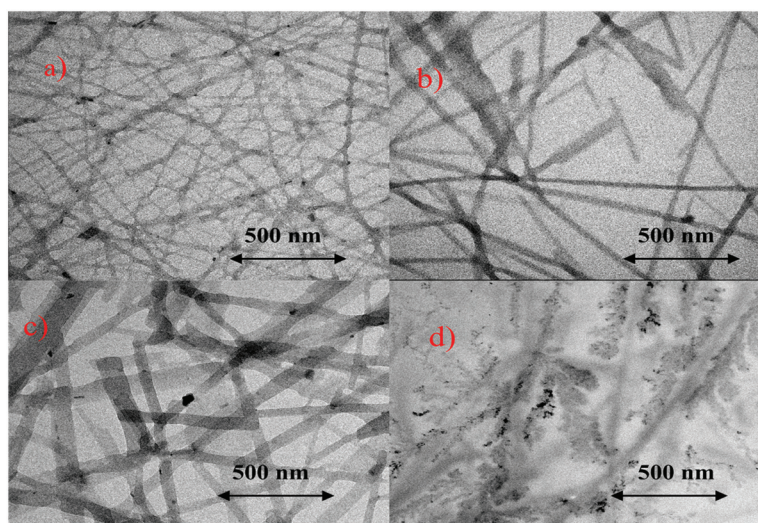


Fig. 4 TEM images of metallogels obtained from (a) Zn-ImF (b) Zn-ImF-AzoPz-1 (c) Zn-ImF-AzoPz-2 (d) Zn-ImF-AzoPz-3 in an alkaline solution of pH \sim 11 : 00.

entangled network of nanofiber structures with an average diameter of \sim ca. 60 nm (Fig. 4b). The TEM image of the Zn-Im-AzoPz-2 coassembly showed a dense network of nanofibers whose diameters are \sim ca. 80 nm wide (Fig. 4c). Notably, the structure of the Zn-Im-AzoPz-3 coassembly was a thin dendrite like morphology, which is different from those of the nanofiber structures obtained from the Zn-ImF and the Zn-ImF-AzoPz-1 and Zn-ImF-AzoPz-2 coassemblies (Fig. 4d). The inner diameter of these dendrite structures was \sim ca. 10 nm. We speculate that the presence of an additional hydroxyl functional group attached to the N-position of the pyrazole ring in the AzoPz-3 unit (see the molecular structure in Fig. 1) might be responsible for the formation of loose dendrite like structures. The hydroxyl group may provide additional opportunity for hydrogen-bonding interaction enhancing supramolecular cross-linking in the self-assembly process and gel formation.

The TEM images demonstrate that the morphology of the coassembled gels could be tuned by changing the structure of the non-gelling AzoPz units. It is also hypothesized that the Zn^{2+} ions cross links and interconnect the gel aggregates to afford the supramolecular hybrid gels.^{27a}

Rheological study

The viscoelastic properties of the metallogel coassemblies formed from Zn-ImF and Zn-ImF-AzoPzs have been investigated by rheological studies at room temperature using freshly prepared samples. The dynamic amplitude sweep rheological experiments conducted on the Zn-ImF and Zn-ImF-AzoPz coassemblies showed that the storage modulus (G') of all the gels are found to be significantly higher than their loss modulus (G''), indicating that the gels are elastic rather than viscous materials (Fig. 5a). Comparative changes in the G'/G''

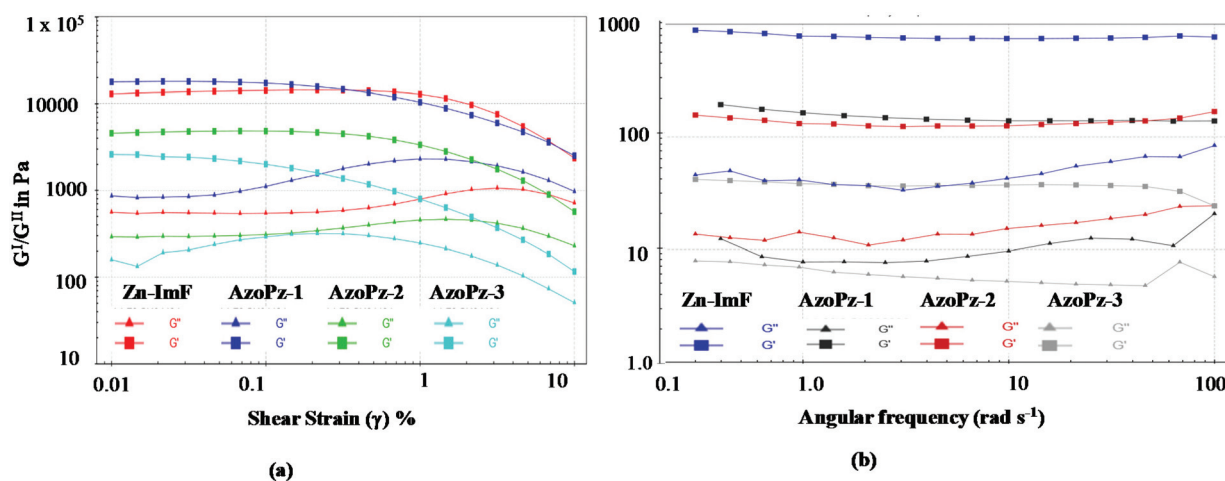


Fig. 5 (a) Dynamic strain amplitude rheological experiment for the Zn-ImF and Zn-ImF-AzoPzs gels; (b) frequency sweep rheological experiment for the Zn-ImF and Zn-ImF-AzoPzs gels.

values also clearly show Zn-ImF and Zn-ImF-AzoPz-1 with the strongest viscoelastic character in these series. Meanwhile, the G' and G'' values of the Zn-ImF-AzoPz-2 and Zn-ImF-AzoPz-3 gels were lower than that of the Zn-ImF gel-*i.e.*, the AzoPzs make the gel network less stiff. Such changes in the viscoelastic properties may be attributed to the slight structural variation of the AzoPz molecular photo-switches, which is in agreement with the TEM images. In the frequency sweep experiment (Fig. 5b), all the metallogel coassemblies were also found to display a higher storage modulus (G') than the loss modulus (G'') which is in agreement with the dynamic amplitude sweep. These observations suggest the formation of viscoelastic metallogels that are fully stable in the detection range of the frequency sweep. In addition, the G' and G'' values also clearly indicated that Zn-ImF-AzoPz-3 has much reduced stiffness compared to those of the Zn-ImF and the Zn-ImF-AzoPz-1-2 gels. Overall, the results imply that the metallogels are fairly tolerant to external force.

Photoisomerization properties of the AzoPzs in solution

The photoswitching properties of the three molecular switches (AzoPz1-3) functionalized with carboxylic acid substituents were studied by using UV-visible spectroscopy. As a representative example, the light-induced photoswitching behavior of AzoPz-1 is shown in Fig. 6a. Before light irradiation, the solution of AzoPz-1 exhibited the characteristic strong absorption band at 341 nm corresponding to the $\pi-\pi^*$ transition of the *trans*-isomer of the AzoPz-1 moiety, whereas the $n-\pi^*$ absorption peak appeared as a relatively weak band at 435 nm.⁴² After

exposing the sample with UV light ($\lambda = 365$ nm), the strong absorption band at 341 nm corresponding to the $\pi-\pi^*$ transition is significantly reduced and blueshifted, whereas the absorbance around 435 nm due to the $n-\pi^*$ transition has increased in intensity and shows a slight redshift (Fig. 6a). Upon irradiation with green light ($\lambda = 530$ nm), the original spectrum for the *trans*-isomer is restored showing a strong absorption band with a maximum centered at 341 nm and a smaller band at 435 nm (Fig. 6b).^{42a,b} These considerable changes in the absorption spectra are indicative of the efficient reversible *trans*-to-*cis* light-induced isomerization of the AzoPz-1 moiety under alternating UV and green light irradiation. The photostationary state (PSS) was reached in 80 s and the *cis*:*trans* ratio in the PSS was found to be 88:12 for AzoPz-1 as determined by UV-vis spectroscopy.

The photoisomerization behavior of the AzoPz-2 and AzoPz-3 molecular switches in solution was examined in a manner similar to that of AzoPz-1 by alternating UV and green light irradiation (Fig. S19 and S20[†]). In general, both AzoPz-2 and AzoPz-3 also showed similar reversible photoisomerization behavior to that of AzoPz-1. Irradiation with 365 nm light leads to a decrease in intensity of the $\pi-\pi^*$ absorbance, whereas the intensity of the $n-\pi^*$ absorbance increases, which is characteristic of isomerization from the thermodynamically stable *trans*-isomer to the *cis*-isomer. The back-switching was examined after irradiation with green light. The intensity of the ~ 345 nm maximum absorption band was fully regained with the original spectrum being recovered with a minimum of 85% of the original intensity, confirming the efficient reversibility of the

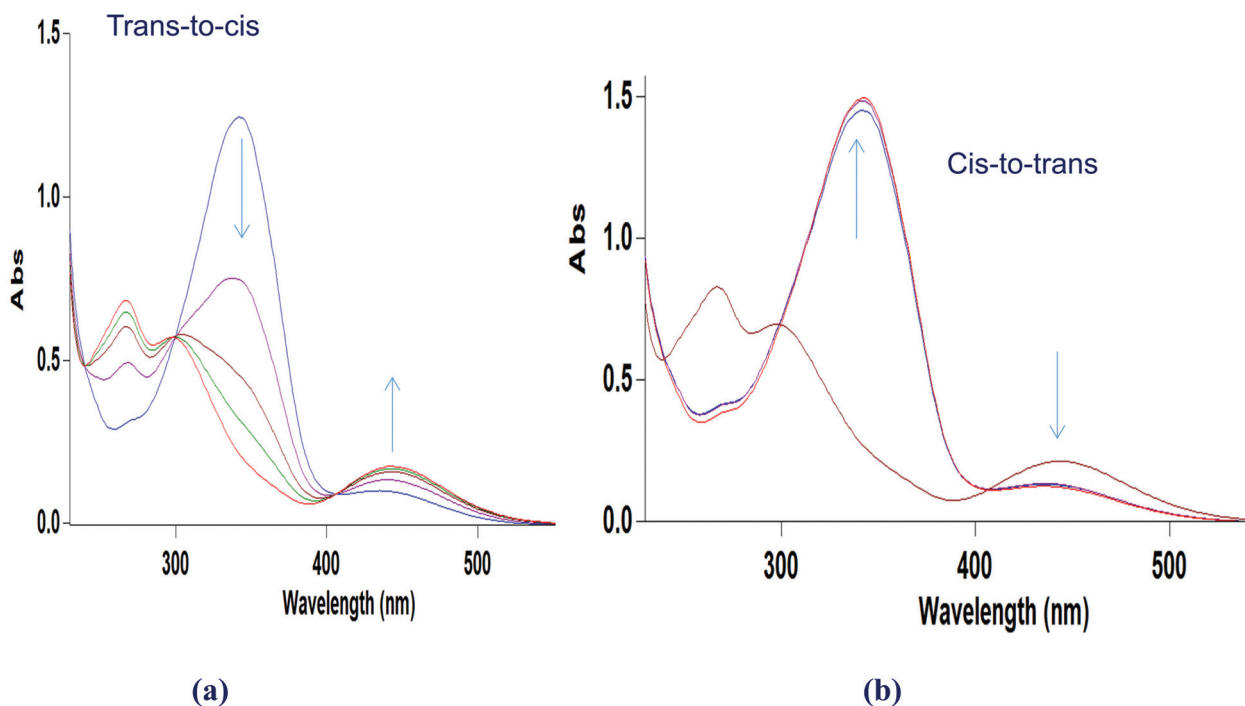


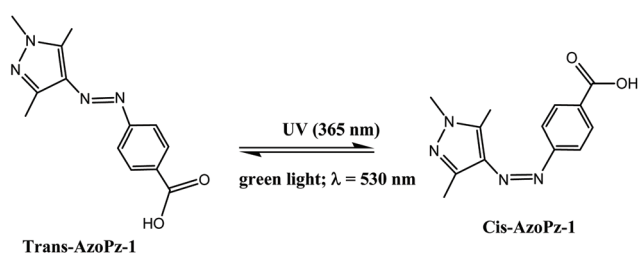
Fig. 6 UV-vis absorption spectra of AzoPz-1: (a) *trans*-to-*cis* upon irradiation at $\lambda = 365$ nm 0–80 s. (b) *cis*-to-*trans* isomerization green light ($\lambda = 530$ nm) 5–180 min.

photochromic process (Fig. S19 and S20 in the ESI†). At the PSS, **AzoPz-2** showed 89% for *trans*-to-*cis* and 94% for *cis*-to-*trans*. On the other hand, **AzoPz-3** showed 90% for *trans*-to-*cis* and 87% for *cis*-to-*trans*.

Photoresponsive properties of metallogel coassemblies

Based on previous studies on photochromic AzoPz containing gels, we hypothesize that the AzoPz units would contribute to the supramolecular interactions responsible for the formation of the entangled nanofibers imaged by TEM through intermolecular π - π stacking, and van der Waals interactions.^{27c,42e} In this context, we supposed that the photo-induced *trans*-to-*cis* isomerization of the AzoPzs should have influence on the self-assembly system through the disturbance of the inter-

molecular interactions resulting in gel-to-sol phase transitions of the Zn-ImF-AzoPz metallogels. An analysis of our results showed that the gels formed from the Zn-ImF-AzoPz coassembly exhibit slow photo-induced reversible gel-to-sol phase transitions. As a representative example the photochemical phase transition of the Zn-ImF-**AzoPz-1** metallogel coassembly is shown in Fig. 7. Upon irradiation with UV light ($\lambda = 365$ nm) the gel formed from the Zn-ImF-**AzoPz-1** coassembly began to collapse, inducing a gradual gel-to-sol transition (2 h). A complete conversion of the gel into the solution took about 4 h (Fig. 5a). The resulting solution could be changed into the gel state upon green light irradiation at $\lambda = 530$ nm for 15 min followed by vortex treatment. The metallogel could also be re-formed by letting the sample rest at room light for 5 h and vortex treatment. This phase transition could be attributed to the photoisomerization of the **AzoPz-1** unit from the planar *trans*-isomer to the twisted *cis*-isomer (Scheme 1), disrupting the gel self-assembly, presumably by destroying the nanofiber organization and π - π stacking. Previous studies by Ravoo and co-workers have shown that the loss of planarity in the *cis*-conformation of the AzoPz containing gels leads to less favorable intermolecular interaction resulting in the formation of a solution.^{42e} Upon green light irradiation ($\lambda = 530$ nm), the planar *trans* conformation is restored and the metallogel is re-formed after vortex treatment as confirmed by the inverted vial test (Fig. 7a). In addition, the gel-to-sol phase transition is accompanied by a color change from yellow to orange, which



Scheme 1 Reversible *trans*-to-*cis* photoisomerization of AzoPz-1.

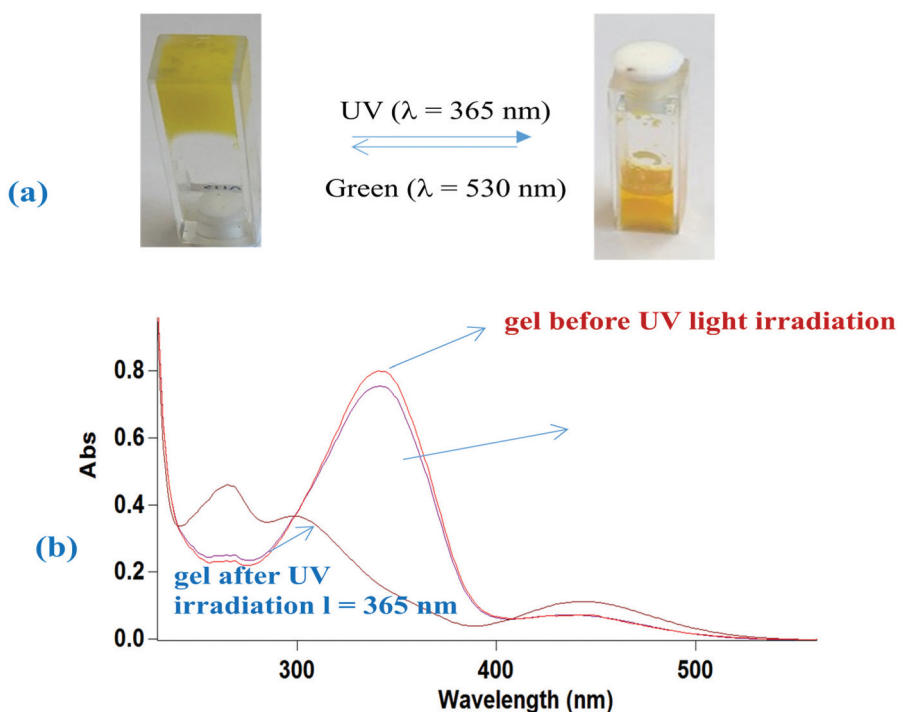


Fig. 7 (a) Photographic image of the reversible photo-induced gel-to-sol phase change of the gel formed by the Zn-Im-**AzoPz-1** coassembly upon alternating UV and green light irradiation; (b) changes in the UV-Vis spectrum of Zn-Im-**AzoPz-1** upon irradiation $\lambda = 365$ nm and recovery of the spectrum after irradiation with green light $\lambda = 530$ nm.

could be attributed to the isomerization of the AzoPz moiety from the *trans* to the *cis*-isomer.

The gel-to-sol switching process was further confirmed by monitoring the UV-vis spectral changes of a DMSO solution of Zn-ImF-AzoPz-1. Before UV light ($\lambda = 365$ nm) irradiation, the Zn-ImF-AzoPz-1 gel exhibits a strong absorption band at 341 nm, arising from the π - π^* transition of the *trans*-form of the AzoPz-1 chromophore (Fig. 7b). Meanwhile, the n - π^* absorption of the AzoPz-1 moiety appeared as a relatively weak band at 440 nm. After exposing a solution of the metallogel coassembly to UV irradiation for 4 min, the absorption band at 340 nm decreased and new absorption bands appeared at 290 nm and 450 nm corresponding to the *cis*-isomer. The light irradiation also caused a blueshift of the π - π^* transition and redshift of the n - π^* transition. Upon green light irradiation for 15 min, the 345 nm absorption band of the *trans* isomer of the AzoPz-1 unit again appeared, and the 290 and 450 nm signals of the *cis* isomer disappeared. Thus, the absorption spectrum of the gel re-produced by green light irradiation, which was identical to that of the initial gel state. These results indicate that the changes in the absorbance intensities of the Zn-ImF-AzoPz-1 coassembly are induced by the *trans*-to-*cis* isomerization of the AzoPz moiety. The conversion efficiency of *cis*-AzoPz-1 can reach *ca.* 80% in the photostationary state within 15 min estimated based on the UV-vis spectra. Additionally, there was no significant change in temperature of the gel during the light-irradiation process. When the orange solution formed by the UV irradiation was stored for 24 h in the dark, the sol state was maintained with no noticeable gel formation. This indicates that the observed gel-to-sol phase transitions proceeded by light-induced photoisomerization.

The Zn-ImF-AzoPz-2 and Zn-ImF-AzoPz-3 gels exhibit similar spectral changes to that of AzoPz-1, but with a slight lower conversion efficiency (see Fig. S19a, b and S20 in the ESI†). Prolonged irradiation with UV light ($\lambda = 365$ nm) induces a partial gel-to-sol phase transition (Fig. S20†). It took 9 h for Zn-ImF-AzoPz-2 and 12 h for Zn-ImF-AzoPz-3 for the

partial gel-to-sol phase transition to occur. The overall long irradiation time needed for the gel-to-sol phase transition to occur could be due to the opaque nature of the multi-component metallogels. These results indicate that the gel-to-sol phase transition slightly depended on the chemical structure of the AzoPz molecular photo-switches.

Fourier-transform infrared spectroscopy (FT-IR) studies

IR spectra were recorded for the pure ImF, the Zn-ImF and the Zn-ImF-AzoPz metallogels (Fig. S21 and S23 in the ESI†). The FTIR spectrum of the pure ImF in the non-gel state showed peaks at 3087 cm^{-1} ($-\text{COOH}$), 3387 cm^{-1} ($-\text{NH}$) and 1609 cm^{-1} for the imidazole ring. Meanwhile, for the Zn-ImF gel, the peak at 3087 cm^{-1} ($-\text{COOH}$) showed a much reduced intensity and the peak at 3387 cm^{-1} ($-\text{NH}$) shifted to 3402 cm^{-1} , suggesting that both the carboxyl O and amino N atoms of the ImF gelator are forming a coordination bond with the Zn^{2+} ion. In addition, the enhanced intensity of the N-H band at 3400 cm^{-1} in the FTIR of the Zn-ImF gel may suggest the presence of hydrogen-bonding interaction that may arise from coordinated water molecules in the self-assembly. Moreover, the 1609 cm^{-1} peak of the imidazole ($-\text{NH}$) stretching shifted to 1600 cm^{-1} indicating the involvement of the imidazole N-H moiety in hydrogen-bonding. The FTIR spectra of the Zn-ImF-AzoPz were almost identical to that of the Zn-ImF gel except for the presence of additional aliphatic region stretching frequencies (Fig. S21 and S23 in the ESI†). These results indicate that the incorporation of the small molecular switches into the structure of the Zn-ImF assembly did not affect the coordination bond that existed between Zn^{2+} ions and the ImF ligand.

X-ray diffraction (XRD) studies

To further provide evidence for the self-assembly process of the different samples, X-ray diffraction studies were performed using vacuum dried xerogels. The XRD patterns of the nano-structured samples are shown in Fig. 8. The XRD results indi-

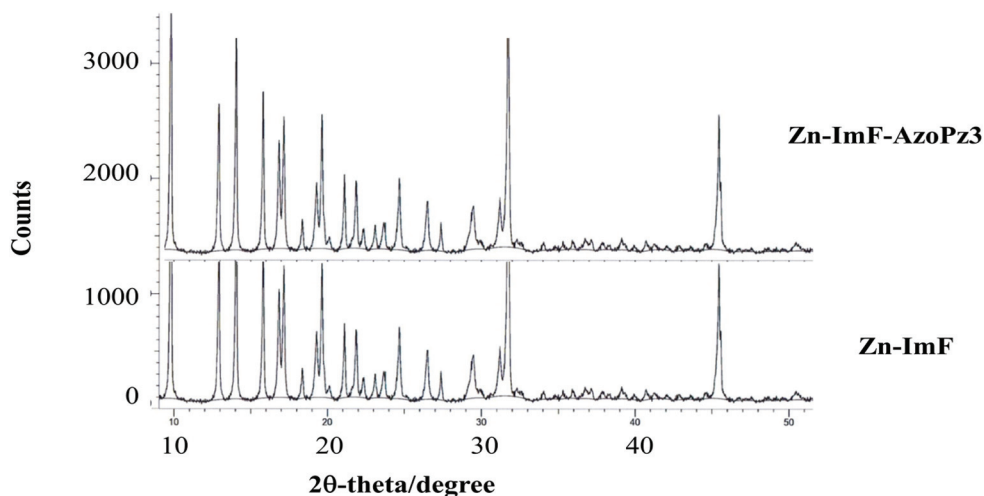


Fig. 8 XRD pattern of the Zn-ImF and Zn-ImF-AzoPz coassembly xerogels.

cated that the samples presented an ordered structure. For the Zn–ImF sample, the presence of a prominent characteristic peak at a d -spacing of 3.63 Å suggested typical π – π stacking interactions in the gelling process. In addition, another peak with a d -spacing of 2.0 Å can be assigned to H-bonds among the Zn–ImF gel network.^{27,46,47}

Furthermore, the XRD of the hybrid gels was studied using Zn–ImF–**AzoPz-3** as a representative example. The results indicated that the addition of the AzoPzs did not significantly change the self-assembly mode of the Zn–ImF metallogel. The XRD pattern of the xerogel of the Zn–ImF–**AzoPz-3** showed a series of peaks at the same position as in the main component Zn–ImF gel (Fig. 8). It may be possible that the hybrid gels are composed of mainly Zn–ImF fiber networks extended by the additional AzoPzs as observed in the TEM images.

Mass spectra [MS (ESI) studies

As described above, the ligand : metal ratio that gives the most stable gel is 2 : 1. This was corroborated by a MS (ESI) study, in which the presence of the 2 : 1 ratio was identified by the formation of an ionized form of the Zn–ImF complex, $[(\text{ImF})_2\text{Zn}]^+$ (see the ESI, Fig. S24[†]). Based on all the above observations, we speculate that ImF likely acts as a tridentate ligand, which binds to Zn^{2+} and forms a hexa-coordination compound of Zn–ImF. The initially formed Zn–ImF metal coordination complex may first self-assemble into fibers and further cross-link the fibers to form intertwined nanofibrillar networks through various non-covalent interactions that include H-bonding interactions and π – π stacking interactions. However, due to the dynamic nature of the coassemblies, attempts to get a clean MS spectra of the hybrid gels were not successful. Spraying a dilute methanol solution of the hybrid gel showed the presence of prominent peaks that belonged to $[(\text{ImF})_2\text{Zn}]^+$ (data not given).

Conclusions

In summary, we have described a simple two/multi-component approach to construct hybrid photoresponsive zinc-based metallogel coassemblies. These gels are formed by mixing an alkaline aqueous solution of an imidazole substituted phenylalanine derivative gelator (ImF) with carboxylic acid functionalized arylazopyrazole (AzoPz) molecular switches and aqueous solutions of zinc salts. We found that all of the AzoPzs could form metallogels with an aqueous solution of the ImF gelator in the presence of Zn^{2+} ions and self-assemble into nanofibers with different morphologies. However, the ImF alone or mixed with the AzoPz photoswitches does not form any gel. This observation indicates that the gelation process is triggered by the Zn^{2+} ions. The results also showed that the gel formation is specific to Zn^{2+} ions. Furthermore, the viscoelastic behavior of the resulting metallogels could be modulated by a structural variation of the small molecular photoswitches. Depending on the functional group linkage of the small molecular switches, the self-assemblies gave nanostructures with slightly different

widths and lengths. Owing to the presence of the AzoPz photo-switchable components, the metallogel assemblies are able to form photoresponsive gels that display a light-triggered phase transition. The metallogel coassemblies undergo a slow reversible light-triggered gel-to-sol phase transition through the *trans*-to-*cis* isomerization of the AzoPz moiety under alternating UV and green light irradiation, resulting in partial or full disassembly of the gels. The reversible gel-to-sol photomodulation of the metallogel coassemblies was achieved through the non-covalent introduction of the carboxylic acid functionalized AzoPz molecular switches. The gel-to-sol phase transition of the metallogels was also found to be slightly dependent on the chemical structure of the AzoPzs; **AzoPz-2** and **AzoPz-3** derivatives took a longer time than **AzoPz-1**. The overall long irradiation time needed for the gel-to-sol phase transition to occur could be due to the opaque nature of the multi-component metallogels. This work provides some inspiration for a convenient fabrication of a new class of photoresponsive coassembled soft materials that combine metal specific properties and light.

Conflicts of interest

The authors declare no conflict of interest.

Acknowledgements

We thank the U.S. National Science Foundation (NSF) for financial support through the Partnership for Research and Education in Materials (PREM) (NSF PREM: Award # 1827820) grant. We thank Dr. Silvina Pagola and Isaiah Ruhl of Old Dominion University for XRD and mass spectroscopy data collection and analysis, respectively. We also thank Dr. Helge Heinrich of the University of Virginia for the collection and analysis of TEM data.

References

- 1 C. Ren, J. Zhang, M. Chen and Z. Yang, *Chem. Soc. Rev.*, 2014, **43**, 7257–7266.
- 2 A. Ajayaghosh, V. K. Praveen and C. Vijayakumar, *Chem. Soc. Rev.*, 2008, **37**, 109–122.
- 3 T. R. Canrinus, W. W. Y. Lee, B. L. Feringa and S. E. J. Bell, *Langmuir*, 2017, **33**, 8805–8812.
- 4 N. Malviya, C. Sonkar, R. Ganguly and S. Mukhopadhyay, *Inorg. Chem.*, 2019, **58**, 7324–7334.
- 5 S. Sarkar, S. Dutta, S. Chakrabarti, P. Bairi and T. Pal, *ACS Appl. Mater. Interfaces*, 2014, **6**, 6308–6316.
- 6 G.-F. Liu, W. Ji, W.-L. Wang and C.-L. Feng, *ACS Appl. Mater. Interfaces*, 2015, **7**, 301–307.
- 7 N. Mehrban, B. Zhu, F. Tamagnini, F. I. Young, A. Wasmuth, K. L. Hudson, A. R. Thomson, M. A. Birchall, A. D. Randall, B. Song and D. N. Woolfson, *ACS Biomater. Sci. Eng.*, 2015, **1**, 431–439.

- 8 S. Das, R. S. Jacob, K. Patel, N. Singh and S. K. Maji, *Biomacromolecules*, 2018, **19**, 1826–1839.
- 9 F. Rodriguez-Llansola, B. Escuder and J. F. Miravet, *J. Am. Chem. Soc.*, 2009, **131**, 11478–11484.
- 10 R. L. Lawrence, Z. E. Hughes, V. J. Cendan, Y. Liu, C.-K. Lim, P. N. Prasad, M. T. Swihart, T. R. Walsh and M. R. Knecht, *ACS Appl. Mater. Interfaces*, 2018, **10**, 33640–33651.
- 11 Y. Zhao, B. Lei, M. Wang, S. Wu, W. Qi, R. Su and Z. He, *J. Mater. Chem. B*, 2018, **6**, 2444–2449.
- 12 P. J. Knerr, M. C. Branco, R. Nagarkar, D. J. Pochan and J. P. Schneider, *J. Mater. Chem.*, 2012, **22**, 1352.
- 13 B. O. Okesola and D. K. Smith, *Chem. Soc. Rev.*, 2016, **45**, 4226–4251.
- 14 O. Owoseni, Y. Zhang, M. Omarova, X. Li, J. Lal, G. L. McPherson, S. R. Raghavan, A. Bose and V. T. John, *J. Colloid Interface Sci.*, 2018, **524**, 279–284.
- 15 J. Karcher and Z. L. Pianowski, *Chem. – Eur. J.*, 2018, **24**, 11605–11610.
- 16 K. Basu, A. Baral, S. Basak, A. Dehsorkhi, J. Nanda, D. Bhunia, S. Ghosh, V. Castelletto, I. W. Hamley and A. Banerjee, *Chem. Commun.*, 2016, **52**, 5045–5048.
- 17 P. R. A. Chivers and D. K. Smith, *Chem. Sci.*, 2017, **8**, 7218–7227.
- 18 V. Castelletto, J. E. McKendrick, I. W. Hamley, U. Olsson and C. Cenker, *Langmuir*, 2010, **26**, 11624.
- 19 N. Malviya, C. Sonkar, B. K. Kundu and S. Mukhopadhyay, *Langmuir*, 2018, **34**, 11575–11585.
- 20 V. Nagarajan and V. R. Pedireddi, *Cryst. Growth Des.*, 2014, **14**, 1895–1901.
- 21 G. S. Thool, K. Narayanaswamy, A. Venkateswararao, S. Naqvi, V. Gupta, S. Chand, V. Vivekananthan, R. R. Koner, V. Krishnan and S. P. Singh, *Langmuir*, 2016, **32**, 4346–4351.
- 22 S. Datta and S. Bhattacharya, *Chem. Soc. Rev.*, 2015, **44**, 5596–5637.
- 23 Y. Cui, B. Chen and G. Qian, *Coord. Chem. Rev.*, 2014, **273–274**, 76–86.
- 24 (a) S. Basak, I. Singh and H.-B. Kraatz, *ChemistrySelect*, 2017, **2**, 451–457; (b) M. Härring and D. D. Diaz, *Chem. Commun.*, 2016, **52**, 13068–13081; (c) S. Saha, J. Bachl, T. Kundu, D. D. Diaz and R. Banerjee, *Chem. Commun.*, 2014, **50**, 3004–3006; (d) T. Feldner, M. Härring, S. Saha, J. Esquena, R. Banerjee and D. D. Diaz, *Chem. Mater.*, 2016, **28**, 3210–3217; (e) B. Sharma, A. Singh, T. K. Sarma, N. Sardana and A. Pal, *New J. Chem.*, 2018, **42**, 6427–6452; (f) S. Basak, I. Singh, A. Banerjee and H.-B. Kraatz, *RSC Adv.*, 2017, **7**, 14461.
- 25 (a) A. Y.-Y. Tam and V. W.-W. Yam, *Chem. Soc. Rev.*, 2013, **42**, 1540–1567; (b) Y. Zhang, B. Zhang, Y. Kuang, Y. Gao, J. Shi, X. Zhang and B. Xu, *J. Am. Chem. Soc.*, 2013, **135**, 5008–5011.
- 26 (a) R. Afrasiabi and H.-B. Kraatz, *Chem. – Eur. J.*, 2015, **21**, 7695–7700; (b) J. Li, I. Cvrtila, M. Colomb-Delsuc, E. Otten and S. Otto, *Chem. – Eur. J.*, 2014, **20**, 15709–15714; (c) E. Borre, S. Bellemin-Laponnaz and M. Mauro, *Chem. – Eur. J.*, 2016, **22**, 18718–18721.
- 27 (a) X. Wang, T. He, L. Yang, H. Wu, J. Yin, R. Shen, J. Xiang, Y. Zhang and C. Wei, *Dalton Trans.*, 2016, **45**, 18438–18442; (b) D. D. Diaz, D. Kuhbeck and R. J. Koopmans, *Chem. Soc. Rev.*, 2011, **40**, 427–448; (c) C.-W. Wei, X.-J. Wang, S.-Q. Gao, G.-B. Wen and Y.-W. Lin, *Dalton Trans.*, 2018, **47**, 13788–13791; (d) A. Biswas, S. Mukhopadhyay, R. S. Singh, A. Kumar, N. K. Rana, B. Koch and D. S. Pandey, *ACS Omega*, 2018, **3**, 5417–5425; (e) Z. Sun, Z. Li, Y. He, R. Shen, L. Deng, M. Yang, Y. Liang and Y. Zhang, *J. Am. Chem. Soc.*, 2013, **135**, 13379–13386.
- 28 Y. Liu, T. Wang, Z. Li and M. Liu, *Chem. Commun.*, 2013, **49**, 4767–4769.
- 29 S. Basak, J. Nanda and A. Banerjee, *Chem. Commun.*, 2014, **50**, 2356–2359.
- 30 (a) V. M. P. Vieira, L. L. Hay and D. K. Smith, *Chem. Sci.*, 2017, **8**, 6981–6990; (b) D. Cornwell, B. O. Okesola and D. K. Smith, *Soft Matter*, 2013, **9**, 8730–8736; (c) W. Edwards and D. K. Smith, *J. Am. Chem. Soc.*, 2013, **135**, 5911–5920.
- 31 L. Ji, G. Ouyang and M. Liu, *Langmuir*, 2017, **33**, 12419–12426.
- 32 Y. Zhang, P. Xue, B. Yao and J. Sun, *New J. Chem.*, 2014, **38**, 5747–5756.
- 33 E. R. Draper and D. J. Adams, *Chem. Commun.*, 2016, **52**, 8196–8199.
- 34 X. Li, J. Fei, Y. Xu, D. Li, T. Yuan, G. Li, C. Wang and J. Li, *Angew. Chem., Int. Ed.*, 2018, **52**, 1–6.
- 35 N. Nandi, S. Basak, S. Kirkham, I. W. Hamley and A. Banerjee, *Langmuir*, 2016, **32**, 13266–13233.
- 36 G.-F. Liu, W. Ji, W.-L. Wang and C.-L. Feng, *ACS Appl. Mater. Interfaces*, 2015, **7**, 301–307.
- 37 M. S. de Luna, V. Marturano, M. Manganelli, C. Santillo, V. Ambrogi, G. Filippone and P. Cerruti, *J. Colloid Interface Sci.*, 2020, **568**, 16–24.
- 38 M. Suzuki, Y. Maruyama and K. Hanabusa, *Tetrahedron Lett.*, 2016, **57**, 3540–3543.
- 39 (a) K. K. Kartha, N. K. Allampally, A. T. Politi, D. D. Prabhu, H. Ouchi, R. Q. Albuquerque, S. Yagai and G. Fernandez, *Chem. Sci.*, 2019, **10**, 752–760; (b) J. Park, L.-B. Sun, Y.-P. Chen, Z. Perry and H.-C. Zhou, *Angew. Chem., Int. Ed.*, 2014, **53**, 5842–5846; G. H. Clever, S. Tashiro and M. Shionoya, *J. Am. Chem. Soc.*, 2010, **132**, 9973–9975; (c) D. Zhang, Y. Nie, M. I. Saha, Z. He, L. Jiang, Z. Zhou and P. J. Stang, *Inorg. Chem.*, 2015, **54**, 11807–11812.
- 40 (a) M. J. Clemente, R. M. Tejedor, P. Romero, J. Fitremann and L. Oriol, *New J. Chem.*, 2015, **39**, 4009–4019; (b) Y.-L. Zhao and J. F. Stoddart, *Langmuir*, 2009, **25**, 8442–8446.
- 41 (a) T. M. Doran, D. M. Ryan and B. L. Nilsson, *Polym. Chem.*, 2014, **5**, 241–248; (b) Y. Huang, Z. Quin, Y. Xu, J. Shi, H. Lin and Y. Zhang, *Org. Biomol. Chem.*, 2011, **9**, 2149–2155.
- 42 (a) C. E. Weston, R. D. Richardson, P. R. Haycock, A. J. P. White and M. J. Fuchter, *J. Am. Chem. Soc.*, 2014, **136**, 11878–11881; (b) R. S. L. Gibson, J. Calbo and

- M. J. Fuchter, *ChemPhotoChem*, 2019, **3**, 372–377; (c) C.-W. Chu and B. J. Ravoo, *Chem. Commun.*, 2017, **53**, 12450–12453; (d) T. Simon, C.-S. Wu, J.-C. Liang, C. Cheng and F.-H. Ko, *New J. Chem.*, 2016, **40**, 2036–2043; (e) C.-W. Chu, L. Stricker, T. M. Kirse, M. Hayduk and B. J. Ravoo, *Chem. – Eur. J.*, 2019, **25**, 6131–6140; (f) K. Ghebreyessus and S. M. Cooper Jr., *Organometallics*, 2017, **36**, 3360–3370.
- 43 (a) S. Engel, N. Möller, L. Stricker, M. Peterlechner and B. J. Ravoo, *Small*, 2018, **14**, 1704287; (b) N. Möller, T. Hellwig, L. Stricker, S. Engel, C. Fallnich and B. J. Ravoo, *Chem. Commun.*, 2017, **53**, 240–243; (c) M. Schnurbus, L. Stricker, B. J. Ravoo and B. Braunschweig, *Langmuir*, 2018, **34**, 6028–6035; (d) S. Lamping, L. Stricker and B. J. Ravoo, *Polym. Chem.*, 2019, **10**, 683–690; (e) J. Moratz, L. Stricker, S. Engel and B. J. Ravoo, *Macromol. Rapid Commun.*, 2018, **39**, 1700256.
- 44 V. Adam, D. K. Prusty, M. Centola, M. Skugor, J. S. Hannam, J. Valero, B. Klöckner and M. Famulok, *Chem. – Eur. J.*, 2018, **24**, 1062–1066.
- 45 A. M. Smith, R. J. Williams, C. Tang, P. Coppo, R. F. Collins and M. L. Turner, *Adv. Mater.*, 2008, **20**, 37–41.
- 46 Q. Hu, Y. Wang, J. Jia, C. Wang, L. Feng, R. Dong, X. Sun and J. Hao, *Soft Matter*, 2012, **8**, 11492–11498.
- 47 I. Ma, J. Jia, T. Yang, G. Yin, Y. Liu, X. Sun and X. Tao, *RSC Adv.*, 2012, **2**, 2902–2908.